SCIENTIFIC REPORTS

OPEN

SUBJECT AREAS:
MECHANISMS OF DISEASE
CANCER STEM CELLS

Received
23 July 2013

Accepted
15 January 2014

Published
17 February 2014

Correspondence and requests for materials should be addressed to R.R.L. (russell.lonser@osumc.edu)

* These authors contributed equally to this work.

Tumor derived vasculogenesis in von Hippel-Lindau disease-associated tumors

Zhengping Zhuang[1]*, Jason M. Frerich[1]*, Kristin Huntoon[1], Chunzhang Yang[1], Marsha J. Merrill[1], Ziedulla Abdullaev[2], Svetlana D. Pack[2], Sharon B. Shively[1], Gordon Stamp[3] & Russell R. Lonser[1,4]

[1]Surgical Neurology Branch, National Institute of Neurological Disorders and Stroke, National Institutes of Health, Bethesda, MD, [2]Laboratory of Pathology, Center for Cancer Research National Cancer Institute, National Institutes of Health, Bethesda, MD, [3]Experimental Pathology Laboratory, Cancer Research UK London Research Institute, Fields, London, [4]Department of Neurological Surgery, The Ohio State University Wexner Medical Center, Department of Neurological Surgery, Columbus, Ohio.

von Hippel-Lindau disease (VHL) patients develop highly vascular tumors, including central nervous system hemangioblastomas. It has been hypothesized that the vascular nature of these tumors is the product of reactive angiogenesis. However, recent data indicate that VHL-associated hemangioblastoma neoplastic cells originate from embryologically-arrested hemangioblasts capable of blood and endothelial cell differentiation. To determine the origin of tumor vasculature in VHL-associated hemangioblastomas, we analyzed the vascular elements in tumors from VHL patients. We demonstrate that isolated vascular structures and blood vessels within VHL-associated hemangioblastomas are a result of tumor-derived vasculogenesis. Further, similar to hemangioblastomas, we demonstrate that other VHL-associated lesions possess vascular tissue of tumor origin and that tumor-derived endothelial cells emerge within implanted *VHL* deficient UMRC6 RCC murine xenografts. These findings further establish the embryologic, developmentally arrested, hemangioblast as the tumor cell of origin for VHL-associated hemangioblastomas and indicate that it is also the progenitor cell for other VHL-associated tumors.

Von Hippel-Lindau disease (VHL) is a progressive multi-system familial tumor syndrome characterized by phenotypically similar vascular tumors in the central nervous system (CNS) and viscera[1]. Characteristic VHL neoplasms include CNS hemangioblastomas, endolymphatic sac tumors, renal cell carcinomas (RCCs), pheochromocytomas and pancreatic cystadenomas[1]. VHL is caused by a germline mutation in the von Hippel-Lindau tumor suppressor gene (*VHL*) located on the short arm of chromosome 3 (3p25–26)[2]. Tumor development occurs after loss of the *wild-type* allele (loss of heterozygosity [LOH])[3–6]. While this *second-hit* is somatic and varies between different tumors in VHL[7], it takes place within a susceptible cell type in an at risk organ system during embryogenesis and results in a consistent tumor phenotype[8–10].

Shared tumor characteristics in VHL can be attributed to a decrease in the production of functional VHL protein (pVHL) in affected tumor cells. pVHL is necessary for the degradation of hypoxia inducible factors ([HIF] HIF-1α and HIF-2α), which in response to tissue hypoxia play a significant role in cellular metabolism, growth and proliferation, as well as induction of angiogenesis and erythropoiesis through the production of downstream factors (e.g., vascular endothelial growth factor [VEGF], platelet derived growth factor [PDGF], erythropoietin [EPO], and endothelin [EDN1])[1,11–13]. Data suggest that constitutively upregulated HIF activity drives the development and progression of the vascular tumors characteristically found in VHL patients[1,13].

Recently, the hemangioblast cell has been identified as giving rise to VHL-associated CNS hemangioblastomas[8–10,14]. Hemangioblast cells are identified by the co-expression of brachyury, Flk-1, and Scl/Tal1[15–17]. Fluorescence-activated cell sorting by known hemangioblast markers ($Tie2^{hi}c\text{-}Kit^{+}CD41^{-}$) *in vitro* yields both endothelial cells and erythrocytes[18,19]. Moreover, VHL-associated tumor cells can evoke blood island formation and differentiate into erythrocytes *in vitro* and *in vivo*, as well as form endothelial cell progeny *in vitro*[8,10]. These findings indicate that VHL-associated hemangioblastomas are not only capable of extramedullary hematopoiesis but potentially blood vessel development.

It had been hypothesized that extensive blood vessel formation in VHL-associated tumors was exclusively the result of reactive angiogenesis within a pseudo-hypoxic (pVHL deficient) cellular environment, and secondary to HIF-induced downstream factor production (VEGF, PDGF, EPO, and END1)[1,13]. However, the discovery of the multipotent hemangioblast as the neoplastic cell in hemangioblastomas suggested that *de novo* formation of new blood vessels directly through stem-like endothelial progenitor cells (hemangioblast cells) could play a role in

tumor blood vessel development. To define the origin of the vasculature in VHL-associated CNS hemangioblastomas and other VHL-associated tumors, we characterized their vasculature *in vitro* and *in vivo*.

Results

To define the vascular features of CNS hemangioblastomas, we systematically examined hemangioblastomas resected from 6 VHL patients and compared the features to normal cerebellum and spinal cord collected at autopsy from 5 patients with VHL and 3 non-VHL controls. CD31 expression, an endothelial specific cell surface marker, highlighted extensive vascular tissue within hemangioblastoma tumors (in contrast with normal cerebellum) (Fig. 1a,b). Hemangioblastoma precursors (defined by CA9 and HIF-2α expression in the absence of HIF-1α expression)[20] were identified within regions of normal cerebellar tissue in autopsy samples from patients with VHL (Fig. 1c,d,e). Both hemangioblastomas and precursor lesions demonstrated the presence of numerous small (10 to 50 micron diameter) unperfused CD31 expressing ring-like vascular structures, indicative of sprouting vessel development with lumen formation (Fig. 1b,f).

To better understand the anatomic relationship of the small unperfused intratumoral vascular structures and characterize the three-dimensional (3D) structure of vasculature in VHL-associated tumor, we performed serial-section 3D immunohistochemical analysis of vessels in tumor. Examination of 3D CD31 expression reconstruction in tumors demonstrated the formation of numerous small isolated islands of vascular tissue (10 to 50 microns) independent from the established vascular network (Figure 1G). To further define potential differences within the vasculature of VHL-associated tumors, we analyzed hemangioblastoma-associated vessels according to size. Immunohistochemical analysis showed larger vessels (greater than 100 microns) expressed Factor VIII with or without CD31 expression, while small vascular structures almost exclusively expressed CD31. Consistent with previous studies, the absence of Factor VIII expression and pronounced CD31 expression in small vascular structures confirmed the presence of immature proliferative endothelial cells within hemangioblastoma tumors (Fig. 2a)[21].

To definitively establish the origin of the small unperfused vascular structures, tissue micro-dissection and extraction was performed of CD31 staining endothelial cells from hemangioblastomas, as previously described (Fig. 2b)[10,22]. Dissected vascular elements demonstrated marked allelic imbalance, confirming LOH (Fig. 2b,c). Blood cell samples and large tumor feeding vessels did not exhibit LOH (Fig. 2c). To further confirm this result, FISH with concurrent

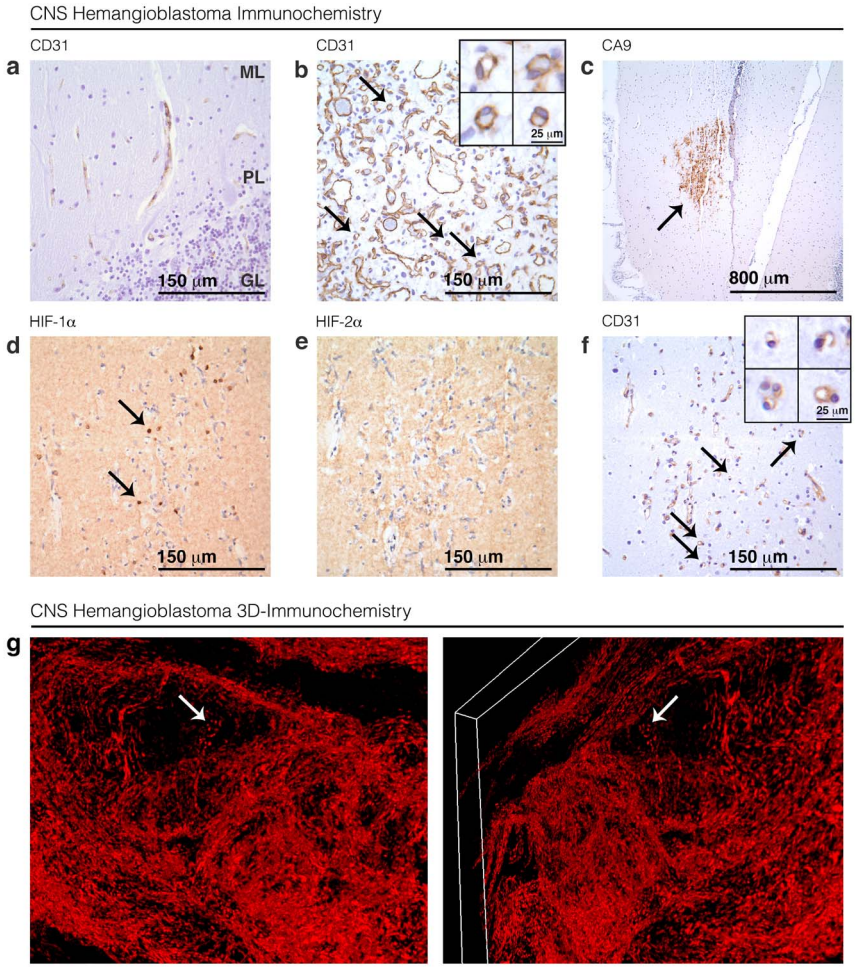

Figure 1 | Characterization of VHL-associated CNS hemangioblastoma tumor vasculature. Immunohistochemistry staining for CD31 of cerebellar tissue demonstrating normal histology with molecular (ML), Purkinje (PL), and granular (GL) layers labeled (a). CNS hemangioblastoma staining for CD31 shows characteristic extensive intratumoral vascular proliferation. Arrows and zoomed-in view indicate small unperfused ring-like tumor vascular structures (10–50 mm) (b). Diffuse CA9 staining demonstrates a hemangioblastoma precursor lesion (arrow) within a region of normal cerebellum (c), confirmed by the presence of HIF-2α positive tumor precursor cells (arrows) (d) and the absence of HIF-1α staining (e). Staining for CD31 of hemangioblastoma precursor lesions also demonstrating the presence of extensive small unperfused ring-like vascular structures (arrows and zoomed-in view) (f). Serial-section 3D immunohistochemical analysis of vessels in VHL-associated tumor demonstrates numerous small isolated islands of CD31 positive vascular tissue (arrows) (g).

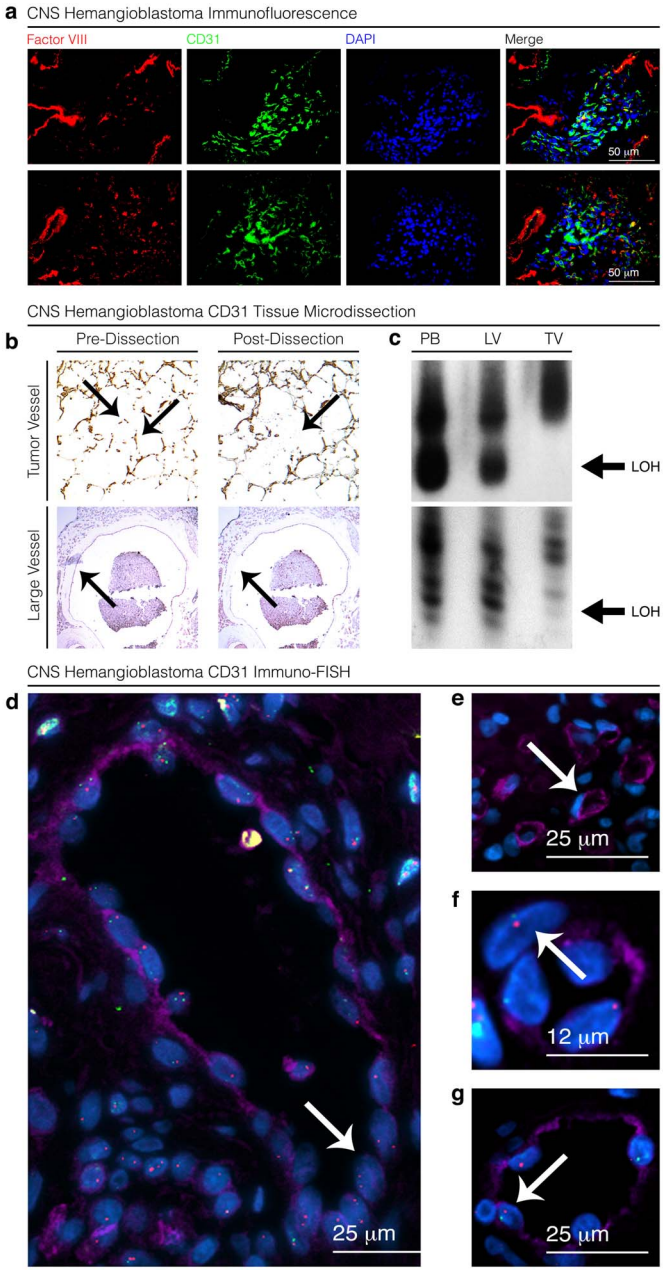

Figure 2 | Analysis of endothelial cell origin in VHL-associated CNS hemangioblastoma. Immunofluorescence staining reveals an absence of Factor VIII expression (red) in small (10–50 mm) CD31 expressing (green) vascular structures and minimal overlap in tumor-associated vessels (a). Micro-dissected vascular structures (arrows) within the tumor (TV), identified by CD31 staining, demonstrate marked allelic imbalance (loss of heterozygosity) (arrows) after amplification with D3S1038 and D3S1110 *VHL*-flanking chromosome 3 primers in comparison to large tumor-feeding vessels (LV) and blood samples (b,c). FISH analysis of CD31 staining endothelial cells (purple) confirming two copies of chromosome 3 (green) or *VHL* (red) (arrows) in most large vessel (100+ μm) endothelial cell nuclei (d) in comparison to loss of one copy of *VHL* (arrows) in nuclei of endothelial cells forming small (10–50 μm) vascular structures (e,f,g). Blots are cropped to enhance clarity and conciseness of presentation.

CD31 immunofluorescence was carried out on hemangioblastoma sections to detect the presence or absence of *VHL* itself. Endothelial cell nuclei within larger vessels (100 microns) displayed retention of both copies of *VHL* (Fig. 2d). Alternatively, small vascular elements (10 to 50 microns) showed one copy of *VHL*, indicating loss of the *wild-type* allele (Fig. 2e,f,g). Complementary LOH and FISH data served to verify that tumor-derived vasculogenesis was taking place within evaluated hemangioblastoma tumors. Large vascular structures also demonstrated some endothelial cells with loss of one copy of *VHL*, consistent with migrating endothelial cells that were recruited during angiogenesis combining with developing *de novo* endothelial cells during tumor blood vessel formation.

To determine if vessels in other VHL-associated tumors were tumor-derived, we examined vascular elements in other VHL-associated lesions collected at autopsy from 5 VHL patients. Micro-dissected endothelial cells from RCCs, kidney cysts, and pancreatic tumors demonstrated characteristic *VHL* LOH in comparison to non-tumor control vessels (Fig. 3a,b). To assess the process of VHL-associated tumor vessel formation *in vivo*, subcutaneous implanted UMRC6 (RCC cell-line with *VHL* deletion) xenografts in NOD. Cg-*Prkdc*^{scid} *Il2rg*^{tm1Wjl}/SzJ mice were surgically extracted at 2 weeks and intratumoral vasculogenesis was analyzed (Fig. 3c). UMRC6 xenografts presumably demonstrated characteristic VHL-associated tumor phenotype with extensive vascularity and clear-cell appearance (Fig. 3d,e). Small vascular structures developing within xenograft lesions were identified by CD31 staining and extracted by micro-dissection (Fig. 3f). Micro-dissected structures demonstrated human genomic (DNA) marker after amplification with *VHL*-flanking chromosome 3 specific primers (D3S1038 and D3S1110), as opposed to control murine muscle tissue that did not amplify (Fig. 3g). Co-localization by immunofluorescence of human specific HLA markers and non-specific CD31 within the xenografts further established the presence of tumor-derived endothelial cells emerging within the tumor, and indicate that the hemangioblast is presumably the tumor cell of origin in VHL-associated tumors other than hemangioblastomas (Fig. 3h,i,j,k).

Discussion

The hemangioblast cell has been identified as the embryologic progenitor cell for both endothelial cells and erythrocytes and proposed as the neoplastic progenitor cell in hemangioblastomas[8–10,14]. These data demonstrate that VHL-associated neoplastic cells maintain the potential to differentiate into endothelial cells, giving direct rise to some tumor blood vessel development. This result should not be confused with recently demonstrated trans-differentiation in glioblastoma and the development of tumor-derived endothelial cells and pericytes[23–25]. The intra- and extra-embryonic mesodermally derived hemangioblast is the origin of coupled vasculogenesis and primitive erythrocyte formation during embryogenesis within the yolk sac and dorsal root of the aorta respectively[18]. Therefore, it is not difficult to conceive that tumors arising from the developmentally arrested hemangioblast are capable of endothelial differentiation.

Tumor progenitor hemangioblasts and RCC tumor cells, of which 90% of sporadic cases possess biallelic *VHL* inactivation, are unable to degrade HIF[26]. Overexpression of HIF and downstream gene activation plays an important role in tumor proliferation, invasion, and angiogenesis[27]. In line with previous reports, our findings indicate that the embryologically arrested pVHL-deficient hemangioblast is the neoplastic progenitor cell in VHL-associated hemangioblastomas and that it also serves as the progenitor cell for other VHL-associated tumors (RCC). Furthermore, based upon both previous and current data, we propose that pVHL-deficient tumor cells develop and progress secondary to constitutively produced proangiogenic factors (VEGF, PDGF, EPO, and EDN1) that stimulate endothelial cell and erythrocyte differentiation, while also inducing angiogenesis within the existent tumor vascular network (Fig. 4a,b)[8,10,13]. In addition, *de novo* endothelial cells can combine with migrating endothelial cells recruited during angiogenesis during tumor blood vessel formation (Fig. 4c). However, at this time we cannot separate integrated tumor-derived endothelial cells from those derived during angiogenesis in terms of function. An in-depth understanding of

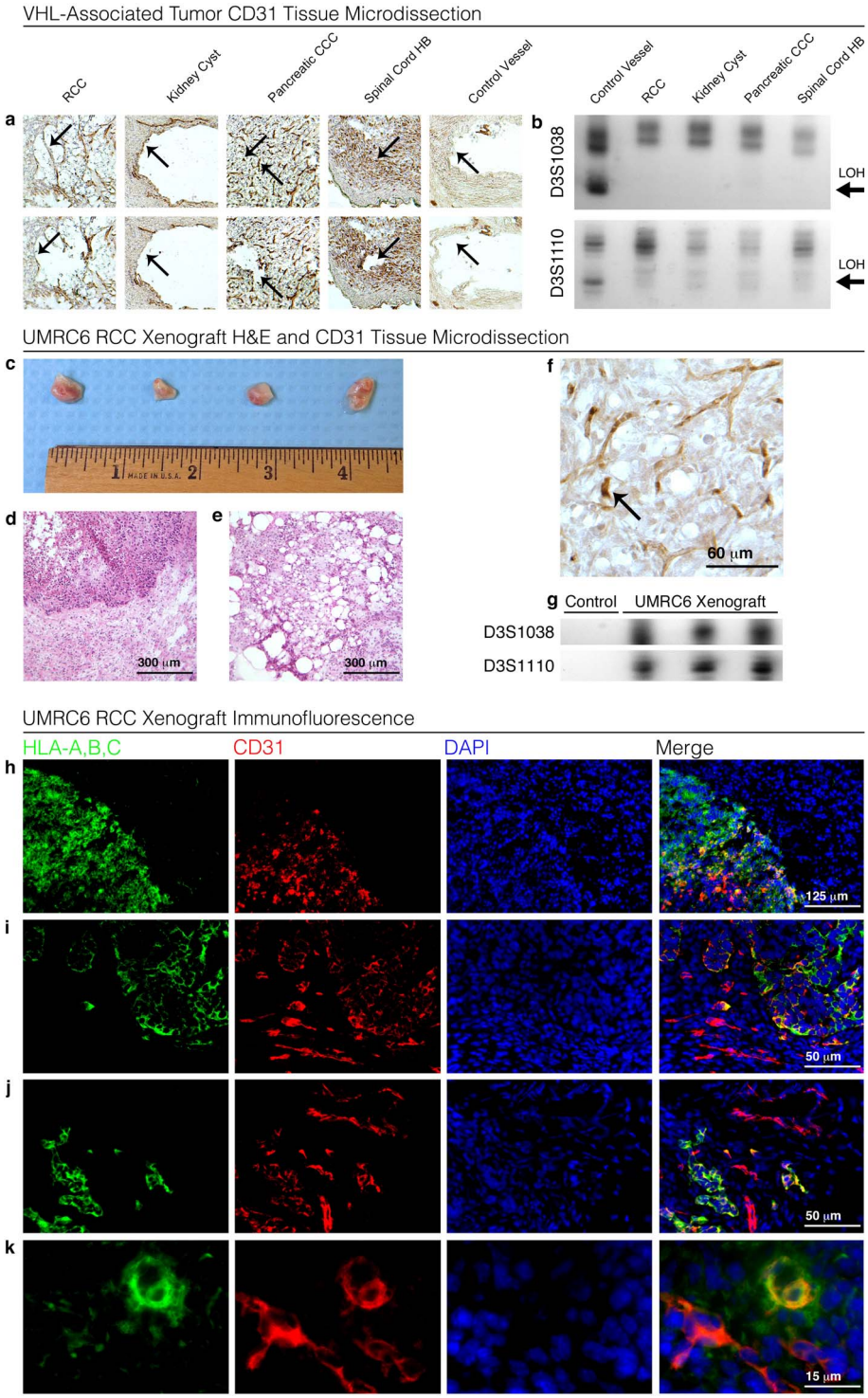

Figure 3 | Evaluation of subcutaneously implanted UMRC6 murine xenografts for intratumoral vasculogenesis. CD31 staining identifying vascular structures (arrows) within RCC, kidney cyst, pancreatic clear cell carcinoma, spinal hemangioblastoma, and non-tumor control vessel (a; upper row). CD31 staining vascular structures were micro-dissected and extracted (arrows) (a; lower row) and demonstrate LOH after amplification with D3S1038 and D3S1110 *VHL*-flanking chromosome 3 primers in comparison to non-tumor control vessel (b). Surgically extracted subcutaneous UMRC6 (renal cell carcinoma cell-line with loss of *VHL*) murine xenografts were assessed for intratumoral vasculogenesis (c). H&E staining of xenografts demonstrates sharp demarcation between human xenograft tumor cells and murine connective tissue (d), as well as characteristic VHL-associated tumor phenotype with the presence of clear-cells and extensive vascular tissue within the xenograft (e). Small vascular structures within the xenograft, identified through CD31 staining, were micro-dissected (f). Micro-dissected vessels demonstrate presence of human genomic (DNA) marker after amplification with D3S1038 and D3S1110, as compared to control murine muscle tissue that did not amplify (g). HLA immunofluorescence (green) clearly demarcated UMRC6 xenograft tumor cells from murine connective tissue cells (h). Co-localization by immunofluorescence for human-specific HLA (MHC class I A, B, and C) (green) and non-specific CD31 (red) confirmed the presence of human endothelial cells emerging within xenografts adjacent to invading murine (non-human) vascular tissue (i,j,k). Blots are cropped to enhance clarity and conciseness of presentation.

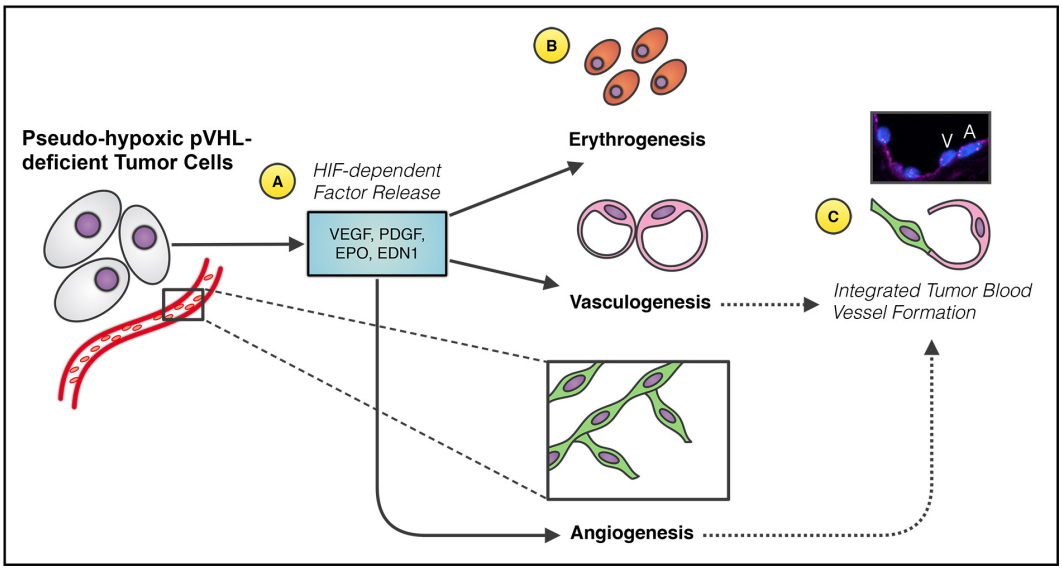

Figure 4 | Proposed schematic depiction of pVHL-deficient tumor cell biology in CNS hemangioblastoma. pVHL-deficient tumor cells (hemangioblasts) in VHL-associated hemangioblastoma, unable to degrade HIF, produce downstream factors vascular endothelial growth factor (VEGF), platelet derived growth factor, erythropoietin, and endothelin secondary to pseudo-hypoxic cellular environment (A). HIF-dependent factor release stimulates hemangioblastoma tumor cells to differentiate into erythrocytes or endothelial cells, while also inducing angiogenesis within the existent tumor vascular network (B). *De novo* endothelial cells (V, vasculogenesis) can combine with migrating endothelial cells (A, angiogenesis), recruited during angiogenesis, during tumor blood vessel formation (C).

vascular tumor biology in VHL-associated tumors will provide additional insight into cancer stem cell biology and tumor progression driven by unregulated HIF expression, as well as highlight the importance of developing novel treatment strategies capable of inhibiting vascular tissue proliferation. More specifically, therapies that exploit the known differentiation potential of the hemangioblast may offer an alternative treatment paradigm for CNS hemangioblastoma.

Methods

VHL tumor samples. Tumor samples were collected at the Surgical Neurology Branch in the National Institute of Neurological Disorders and Stroke (NINDS) under an instutition-approved protocol (NIH 03-N-164).

Immunohistochemistry staining. Tissues were fixed in Histochoice (Amresco) with 0.1% Triton X-100 (Research Products International). Detection of antibody was performed using the Vectastain ABC reagent (1 : 50) and DAB (Vector Laboratories). Sections were counterstained with Mayer's hematoxylin (Sigma-Aldrich). Primary antibodies were as follows: anti-CD31 (1 : 200, Dako).

Immunofluorescence staining and flourescence in situ hybridization (FISH). Slides were fixed with Histochoice (Amresco) and labeled overnight with primary antibodies. Nuclei of cells were counterstained with DAPI (Sigma-Aldrich). Staining was visualized with a Zeiss LSM 510 confocal microscope (Carl Zeiss). Primary antibodies were as follows: anti-factor VIII (1 : 200, Sigma-Aldrich), anti-CD31 (1 : 200, Dako), and anti-HLA Class I ABC (1 : 200, MBL International). For interphase FISH analysis, BAC clone RP11-438J1 (210 kb) including the entire *VHL* gene from the 3p25.3 region was used. The VHL BAC DNA probe labeled by SpectrumOrange was purchased from Empire Genomics. Centromere enumeration probe for chromosome 3 (CEP3) labeled with SpectrumGreen was purchased from Abbott Molecular. FISH assays were performed on 5 micron Formalin-Fixed-Paraffin-Embedded (FFPE) tumor sections using laboratory standardized protocol with slight modification[26]. Denaturation of target DNA on slides was carried out by co-denaturation of the probe and target DNA at 73°C in HYBrite (Abbott Molecular) for 5 min followed by overnight hybridization at 37°C. The next day, slides were washed at 72°C in 0.4× SSC/0.3% Tween-20 for 2 min and then in 2× SSC/0.1% Tween-20 at room temperature for 1 min. Slides were counterstained, mounted with DAPI/Antifade (Vector Laboratories) and analyzed on the BioView Duet-3 fluorescent scanning station using 63× oil objective and DAPI/FITC/Rhodamine single band filters (Semrock).

Three-dimensional immunohistochemistry. Serial sections were cut at 8.0-μm thickness. After staining (anti-CD31), individual micrographs were collected and stacked. Images were captured using a Yokogawa spinning-disk confocal on a Nikon TE2000U inverted microscope with a 1003 Plan Apo NA 1.4 objective lens, a Hamamatsu ORCA ER-cooled CCD camera, and MetaMorph software. Image stacks were aligned, analyzed, and visualized using freeware Reconstruct software (SynapseWeb).

DNA extraction and loss of heterozygosity testing. Tissue dissection was performed as previously described[27,28]. Samples were screened for loss of heterozygosity (LOH) with two polymorphic markers D3S1038 and D3S1110 flanking the VHL gene as previously described with minor modifications[6].

Cell culture and tumor xenografts. Human renal cell carcinoma cell line UMRC6 was maintained in Dulbecco's modified essential medium (Gibco) supplemented with 10% fetal bovine serum and Insulin-Transferrin-Selenium-Ethanolamine (Gibco). Animal experiments were approved for use and care of animals under the protocol guidelines of the National Institutes of Health Animal Care and Use Committee. NOD. Cg-*Prkdc*^{scid} *Il2rg*^{tm1Wjl}/SzJ mice (aged 6 to 8-wk, male) were purchased from Jackson Laboratories. 10^7 UMRC6 cells in 200 μL PBS were injected subcutaneously. Tumors were excised and processed for morphological study two weeks after initial implantation.

1. Lonser, R. R., Glenn, G. M., Walther, M. *et al.* Von Hippel-Lindau disease. *Lancet* **361**, 2059–2067 (2003).
2. Latif, F., Tory, K., Gnarra, J. *et al.* Identification of the von Hippel-Lindau disease tumor suppressor gene. *Science* **260**, 1317–1320 (1993).
3. Kaelin, W. G. Molecular basis of the VHL hereditary cancer syndrome. *Nat. Rev. Cancer* **2**, 673–682 (2002).
4. Zbar, B., Kishida, T., Chen, F. *et al.* Germline mutations in the Von Hippel-Lindau disease (VHL) gene in families from North America, Europe, and Japan. *Hum. Mutat.* **8**, 348–357 (1996).
5. Wait, S. D., Vortmeyer, A. O., Lonser, R. R. *et al.* Somatic mutations in VHL germline deletion kindred correlate with mild phenotype. *Ann. Neurol.* **55**, 236–240 (2004).
6. Lee, J. Y., Dong, S. M., Park, W. S. *et al.* Loss of heterozygosity and somatic mutations of the VHL tumor suppressor gene in sporadic cerebellar hemangioblastomas. *Cancer Res.* **58**, 504–508 (1998).
7. Gläsker, S., Sohn, T.-S., Okamoto, H. *et al.* Second hit deletion size in von Hippel-Lindau disease. *Ann. Neurol.* **59**, 105–110 (2006).
8. Park, D. M., Zhuang, Z., Chen, L. *et al.* Von Hippel-Lindau disease-associated hemangioblastomas are derived from embryologic multipotent cells. *PLoS Med.* **4**, e60 (2007).
9. Gläsker, S., Li, J., Xia, J. B. *et al.* Hemangioblastomas share protein expression with embryonal hemangioblast progenitor cell. *Cancer Res.* **66**, 4167–4172 (2006).
10. Vortmeyer, A. O., Frank, S., Jeong, S.-Y. *et al.* Developmental arrest of angioblastic lineage initiates tumorigenesis in von Hippel-Lindau disease. *Cancer Res.* **63**, 7051–7055 (2003).

11. Maxwell, P. H., Wiesener, M. S., Chang, G. W. *et al.* The tumour suppressor protein VHL targets hypoxia-inducible factors for oxygen-dependent proteolysis. *Nature* **399**, 271–275 (1999).
12. Keith, B., Johnson, R. S. & Simon, M. C. HIF1α and HIF2α: sibling rivalry in hypoxic tumour growth and progression. *Nat. Rev. Cancer* **12**, 9–22 (2012).
13. Rathmell, W. K. & Simon, M. C. VHL: oxygen sensing and vasculogenesis. *J. Thromb. Haemost.* **3**, 2627–2632 (2005).
14. Vortmeyer, A. O., Gnarra, J. R., Emmert-Buck, M. R. *et al.* Von Hippel-Lindau gene deletion detected in the stromal cell component of a cerebellar hemangioblastoma associated with von Hippel-Lindau disease. *Hum. Pathol.* **28**, 540–543 (1997).
15. Choi, K., Kennedy, M., Kazarov, A., Papadimitriou, J. C. & Keller, G. A common precursor for hematopoietic and endothelial cells. *Development* **125**, 725–732 (1998).
16. Huber, T. L., Kouskoff, V., Fehling, H. J., Palis, J. & Keller, G. Haemangioblast commitment is initiated in the primitive streak of the mouse embryo. *Nature* **432**, 625–630 (2004).
17. Yoshimoto, M. & Yoder, M. C. Developmental biology: Birth of the blood cell. *Nature* **457**, 801–803 (2009).
18. Lancrin, C., Sroczynska, P., Stephenson, C. *et al.* The haemangioblast generates haematopoietic cells through a haemogenic endothelium stage. *Nature* **457**, 892–895 (2009).
19. Vogeli, K. M., Jin, S.-W. & Martin, G. R. Stainier DYR. A common progenitor for haematopoietic and endothelial lineages in the zebrafish gastrula. *Nature* **443**, 337–339 (2006).
20. Shively, S. B., Falke, E. A., Li, J. *et al.* Developmentally arrested structures preceding cerebellar tumors in von Hippel-Lindau disease. *Mod. Pathol.* **24**, 1023–1030 (2011).
21. Wang, D., Stockard, C. R., Harkins, L. *et al.* Immunohistochemistry in the evaluation of neovascularization in tumor xenografts. *Biotech Histochem.* **83**, 179–189 (2008).
22. Merrill, M. J., Edwards, N. A. & Lonser, R. R. Hemangioblastoma-associated mast cells in von Hippel-Lindau disease are tumor derived. *Blood* **121**, 859–860 (2013).
23. Wang, R., Chadalavada, K., Wilshire, J. *et al.* Glioblastoma stem-like cells give rise to tumor endothelium. *Nature* **468**, 829–833 (2010).
24. Soda, Y., Marumoto, T., Friedmann-Morvinski, D. *et al.* Transdifferentiation of glioblastoma cells into vascular endothelial cells. *Proc. Natl. Acad. Sci. U.S.A.* **108**, 4274–4280 (2011).
25. Cheng, L., Huang, Z., Zhou, W. *et al.* Glioblastoma stem cells generate vascular pericytes to support vessel function and tumor growth. *Cell* **153**, 139–152 (2013).
26. Keith, B., Johnson, R. S. & Simon, M. C. HIF1α and HIF2α: sibling rivalry in hypoxic tumour growth and progression. *Nat. Rev. Cancer* **12**, 9–22 (2011).
27. Shuin, T., Kondo, K., Torigoe, S. *et al.* Frequent somatic mutations and loss of heterozygosity of the von Hippel-Lindau tumor suppressor gene in primary human renal cell carcinomas. *Cancer Res.* **54**, 2852–2855 (1994).
28. Pack, S. D. & Zhuang, Z. Fluorescence in situ hybridization: application in cancer research and clinical diagnosis. *Methods Mol. Med.* **50**, 35–50 (2001).

Author contributions

J.F., K.H., C.Y., M.M., Z.A., S.P. and S.S. performed experiments; Z.Z., J.F., K.H., M.M., S.P. and R.L. analyzed results and made the figures; Z.Z., J.F., K.H. and R.L. designed the research and wrote the paper. Presented as an oral presentation at the AANS/CNS 10th Biennial Satellite Tumor Symposium in New Orleans, LA, April 26–27, 2013.

Additional information

Competing financial interests: The authors declare no competing financial interests.

How to cite this article: Zhuang, Z.P. *et al.* Tumor derived vasculogenesis in von Hippel-Lindau disease-associated tumors. *Sci. Rep.* **4**, 4102; DOI:10.1038/srep04102 (2014).